PERGAMON

International Journal of Rock Mechanics & Mining Sciences 37 (2000) 1239–1246

International Journal of
Rock Mechanics
and Mining Sciences

www.elsevier.com/locate/ijrmms

The strength of hard-rock pillars

C.D. Martin[a,*], W.G. Maybee[b]

[a] Department of Civil & Environmental Engineering, University of Alberta, Edmonton, Alberta, Canada T6G 2G7
[b] Geomechanics Research Centre, Laurentian University, Fraser Building F217, Ramsey Lake Road Sudbury, ON, Sudbury, Canada P3E 2C6

Accepted 14 April 2000

Abstract

Observations of pillar failures in Canadian hard-rock mines indicate that the dominant mode of failure is progressive slabbing and spalling. Empirical formulas developed for the stability of hard-rock pillars suggest that the pillar strength is directly related to the pillar width-to-height ratio and that failure is seldom observed in pillars where the width-to-height ratio is greater than 2. Two-dimensional finite element analyses using conventional Hoek–Brown parameters for typical hard-rock pillars (Geological Strength Index of 40, 60 and 80) predicted rib-pillar failure envelopes that did not agree with the empirical pillar-failure envelopes. It is suggested that the conventional Hoek–Brown failure envelopes over predict the strength of hard-rock pillars because the failure process is fundamentally controlled by a cohesion-loss process in which the frictional strength component is not mobilized. Two-dimensional elastic analyses were carried out using the Hoek-Brown brittle parameters which only relies on the cohesive strength of the rock mass. The predicted pillar strength curves were generally found to be in agreement with the observed empirical failure envelopes.

1. Introduction

Pillars can be defined as the in situ rock between two or more underground openings. Hence, all underground mining methods utilize pillars, either temporary or permanent, to safely extract the ore. In coal mines rectangular pillars are often designed in regular arrays such that should a single pillar inadvertently fail the load could be transferred to adjacent pillars causing these to be overloaded. This successive overloading process can lead to an unstable progressive "domino" effect whereby large areas of the mine can collapse. This type of failure occurred in 1960 and resulted in the collapse of 900 pillars in the Coalbrook coal mine in South Africa and the loss of 437 lives. Recently, Salamon [1] summarized the extensive research into coal-pillar design that followed the Coalbrook disaster. The key element that has been used since 1960 for the successful design of coal pillars is "back-calculation", an approach that has been used extensively in geotechnical engineering [2]. This approach has led to the development of empirical pillar strength formulas but can only be implemented by observing and documenting failed pillars.

The design of hard-rock pillars has not received the same research attention as coal pillar design. This is partly because fewer mines operate at depths sufficient to induce the stresses required to cause hard rocks to fail, and in hard-rock mining pillar and mining geometries are irregular making it difficult to establish actual loads. Nonetheless as mining depth increases the potential for the failure of hard-rock pillars also increases. This paper focuses on the strength of hard-rock pillars, particularly rib-pillars, and presents a stability criterion that can be used to establish hard-rock pillar geometries.

2. Empirical pillar strength formulas

Following the Coalbrook disaster, a major coal-pillar research program was initiated in South Africa. One of the main objectives of this research was to establish the in situ strength of coal pillars. Using the back-calculation approach Salamon and Munro [9] analyzed 125 case histories involving coal-pillar collapse and proposed that the coal-pillar strength could be

*Corresponding author. Tel.: +1-780-492-2332; fax: +1-780-492-8198.

E-mail address: dmartin@civil.ualberta.ca (C.D. Martin).

1365-1609/00/$ - see front matter
PII: S1365-1609(00)00032-0

Table 1
Summary of empirical strength formula for hard-rock pillars where the pillar width and height is in metres.

Reference	Pillar strength formulas (MPa)	σ_c (MPa)	Rock mass	No. of pillars
[3]	$133\frac{W^{0.5}}{H^{0.75}}$	230	Quartzites	28
[4]	$65\frac{W^{0.46}}{H^{0.66}}$	94	Metasediments	57
[5]	$35.4(0.778+0.222\frac{W}{H})$	100	Limestone	14
[6]	$0.42\sigma_c\frac{W}{H}$	—	Canadian Shield	23
[7]	$74(0.778+0.222\frac{W}{H})$	240	Limestone/Skarn	9
[8]	$0.44\sigma_c(0.68+0.52\kappa)$	—	Hard rocks	178[a]

[a] Database compiled from published sources including those listed in this table.

adequately determined using the power formula

$$\sigma_p = K\frac{W^{\alpha}}{H^{\beta}}, \quad (1)$$

where σ_p (MPa) is the pillar strength, K (MPa) is the strength of a unit volume of coal, and W and H are the pillar width and height in metres, respectively. The notion that the strength of a rock mass is to a large part controlled by the geometry of the specimen, i.e., the width-to-height ratio, has since been confirmed by extensive laboratory studies, e.g., [10]. The data from the 125 case studies gave the following values for the parameters in Eq. (1): $K = 7.176$ MPa, $\alpha = 0.46$ and $\beta = 0.66$. According to Madden [11] and Salamon [1] Eq. (1) has been applied extensively to the design of pillar layouts in South Africa since its introduction in 1967. While it is tempting to apply Eq. (1) to other pillar designs, it must be remembered that Eq. (1) was developed for room and pillar mining of horizontal coal seams and that the value of K is only typical for South African coal.

One of the earliest investigations into the design of hard-rock pillars was carried out by Hedley and Grant [3]. They analyzed 28 rib-pillars (3 crushed, 2 partially failed, and 23 stable) in massive quartzites and conglomerates in the Elliot Lake room and pillar uranium mines. These pillars were formed with the long-axis of the rib-pillar parallel to the dip direction of the quartzites. They concluded that Eq. (1) could adequately predict these hard-rock pillar failures but that the parameters needed to be modified to

$$\sigma_p = K\frac{W^{0.5}}{H^{0.75}}, \quad (2)$$

where the units are the same as Eq. (1). The value of K in Eq. (2) was initially set as 179 MPa but later reduced to 133 MPa [12].

Since 1972 there have been several additional attempts to establish hard-rock pillar strength formulas, using the "back-calculation" approach (Table 1). Inspection of Table 1 reveals that the best-fit formulas for the observed pillar failures take the form of either a power- or linear-type equation, and that these equations

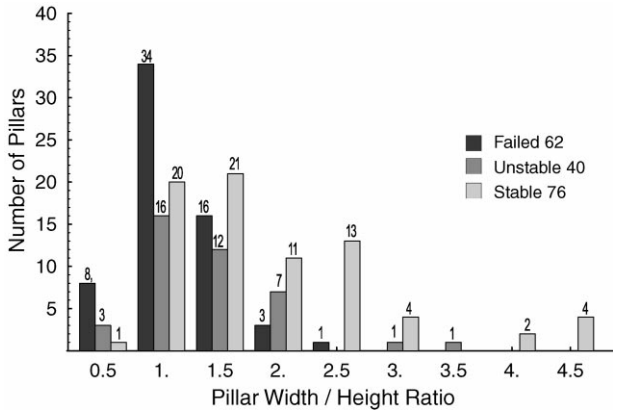

Fig. 1. Summary of the failed, transitional and stable pillars used to establish the pillar strength formulas in Table 1.

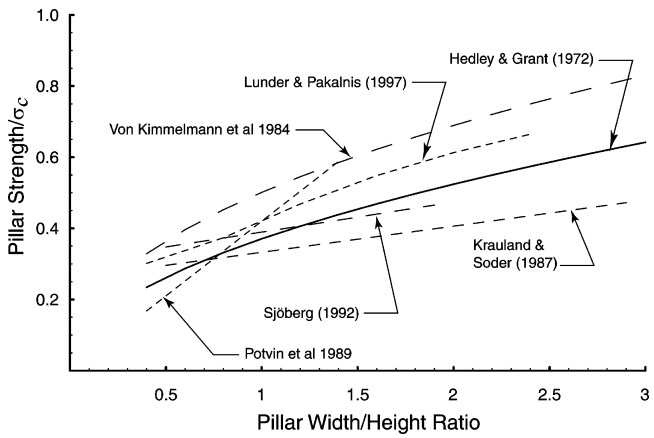

Fig. 2. Comparison of the empirical pillar strength formulas in Table 1.

have been used to predict the pillar strength for a wide range of pillar shapes and rock mass strengths as indicated by the unconfined compressive strength (94−240 MPa). Fig. 1 provides a summary of the "failed", "unstable" and "stable" classes of pillars that were used to establish the pillar strength formulas in Table 1. Fig. 2 shows the predicted pillar strength from the various formulas using a pillar height of 5 m. The

pillar strengths in Fig. 2 have been normalized to the laboratory uniaxial compressive strength (σ_c). As shown in Fig. 2 the formulas predict very similar strengths, particularly for the pillar W/H ratio between 0.5 and 2.5, the range over which all of the pillar failures occur (see Fig. 1).

The stress magnitudes used to establish the pillar strengths formulas in Table 1, which were determined using either the tributary area method, or two and three dimensional elastic analyses, represent either the average maximum pillar stress or the maximum stress at the center of the pillar. In all cases, except the formula presented by Lunder and Pakalnis [8], the pillar-strength formulas ignore the effect of σ_3 and rely on a simple stress to strength ratio based on the maximum pillar stress and the uniaxial compressive strength. While Lunder and Pakalnis [8] attempt to include the effect of σ_3 through their parameter κ (see Table 1) their formula predicts similar strengths to the other formulas in Table 1 (Fig. 2). Hence the effect of σ_3 is essentially ignored by the empirical formulas to match the observed failures. This is similar to tunnel stability observations in South African mines where the stability is expressed as a simple stress to strength (σ_1/σ_c) ratio [13].

The elastic stress distribution in pillars is a function of the pillar geometry. These distributions can readily be determined through numerical computer programs. Lunder and Pakalnis [8] examined the stress distribution in hard-rock pillars in Canadian mines and proposed that the average confinement in a pillar could be expressed in terms of the ratio of σ_3/σ_1. They then expressed this ratio in terms of the pillar width and pillar height as

$$\frac{\sigma_3}{\sigma_1} = 0.46\left[\log\left(\frac{W}{H} + 0.75\right)\right]^{\frac{1.4}{(W/H)}}. \tag{3}$$

Fig. 3 illustrates Eq. (3) and shows that the confinement in pillars increases significantly beyond a pillar W/H ratio of 1. Recently, Maybee [14] showed however, that the rate of increase is a function of k, the ratio of the far-field horizontal stress σ_1 and σ_3 (Fig. 3). Fig. 3 shows that beyond a pillar W/H ratio of 1 the effect of k is significant but for pillar W/H ratios less than 1 the effect of k can be ignored.

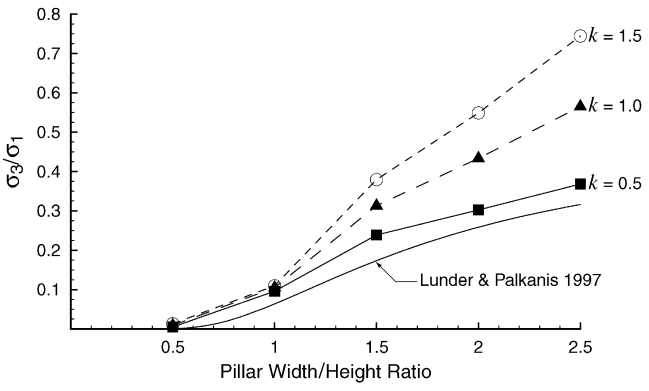

Fig. 3. The increase in confinement at the center of the pillar as a function of k, the ratio of the far-field maximum horizontal stress and vertical stress. The predicted effect of confinement using Eq. (3) is also shown.

The strength of a rock mass is usually described in terms of a constant cohesive component and a normal-stress or confinement-dependent component. Hence for pillars with W/H ratios greater than 1, the strength should increase as the confining stress increases. In the next section the Hoek–Brown failure criterion is used to investigate the effect of confinement on pillar strength.

3. Pillar and rock mass strength

One of the most widely used empirical failure criteria is the Hoek–Brown criterion [13]. Since its introduction in 1980 the criterion has been modified several times, most recently in 1997 [15]. The generalized form of the criterion for jointed rock masses is defined by

$$\sigma_1 = \sigma_3 + \sigma_{ci}\left(m_b\frac{\sigma_3}{\sigma_{ci}} + s\right)^a, \tag{4}$$

where σ_1 and σ_3 are the maximum and minimum effective stresses at failure, respectively, m_b is the value of the Hoek–Brown constant m for the rock mass, and s and a are constants which depend upon the characteristics of the rock mass, and σ_{ci} is the uniaxial compressive strength of the intact rock pieces. For hard-rock masses, Hoek and Brown [15] recommend a value of 0.5 for a. In order to use the Hoek–Brown criterion for estimating the strength and deformability of jointed rock masses, "three properties" of the rock mass have to be estimated. These are: (1) the uniaxial compressive strength σ_{ci} of the intact rock pieces in the rock mass; (2) the Hoek–Brown constant m_i for these intact rock pieces; and (3) the Geological Strength Index (GSI) for the rock mass. The GSI was introduced by Hoek and Brown [15] to provide a system for estimating the reduction in the rock mass strength for different geological conditions. The GSI can be related to either of the commonly used rock-mass classification systems, e.g., the modified rock-mass quality index Q' defined as

$$Q' = \frac{RQD}{J_n} \times \frac{J_r}{J_a}, \tag{5}$$

where RQD is the rock quality designation, J_n is the joint set number, J_r is the joint roughness number, J_a is the joint alteration number or the rock mass rating RMR. Hoek and Brown [15] suggested that GSI can be related to Q' by

$$GSI = 9\ln Q' + 44 \tag{6}$$

and to RMR by

$$GSI = RMR_{89} - 5, \tag{7}$$

where RMR_{89} has the Groundwater rating set to 15 and the Adjustment for Joint Orientation set to zero. The parameters m_b and s can be derived from GSI by the following:

$$m_b = m_i \exp\left(\frac{GSI - 100}{28}\right), \tag{8}$$

$$s = \exp\left(\frac{GSI - 100}{9}\right). \tag{9}$$

The Elliot Lake uranium orebody was actively mined from the early 1950s through to the mid-1990s. The shallow (10−15°) dipping tabular deposit was characterized by uranium bearing conglomerates separated by massive quartzite beds 3−30 m thick [3,16]. Mining was carried out using room-and-pillar and stope-and-pillar methods with long (76 m) narrow rib-pillars formed in the dip direction. The rock mass quality of the pillars ranged from good to very good ($Q = 10-100$)(C. Pritchard, pers. comm.). Seismic surveys carried out across various pillars indicated that at the core of stable pillars the P-wave velocity averaged about 6 km/s while at the edge of the pillars the P-wave velocity dropped to 5.5 km/s [16]. Barton and Grimstad [17] proposed the following correlation between seismic compressional wave velocity and rock mass quality Q for non-porous rocks:

$$Q = 10\frac{V_p - 3500}{1000}, \tag{10}$$

where V_p is the P-wave velocity in m/s. This relationship is shown in Fig. 4 along with the results from the pillar velocity surveys. These results also support the notion that the pillars were excavated in a very good-quality rock mass. These descriptions and measurements indicate that the rock mass strength can be characterized by a GSI value of 80 (very good category), which was used to establish the parameters required for the Hoek−Brown failure criterion (Table 2).

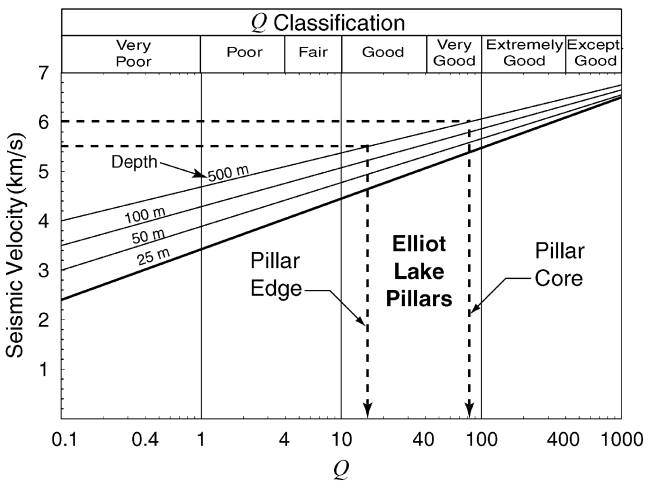

Fig. 4. Estimation of the rock mass quality from pillar seismic surveys.

Table 2
Parameters used in the Phase2 modelling to estimate the strength of the Elliot Lake pillars, assuming an elastic brittle response.

Parameter	Description/value
Rock-type	Quartzite, Conglomerate
Insitu stress	$\sigma_1 = 2\sigma_3$ and $\sigma_2 = 1.66\sigma_3$
	$\sigma_3 = 0.028$ MPa/m
Intact rock strength	$\sigma_{ci} = 230$ MPa
Geological Strength Index	$GSI = 80$
Hoek−Brown constants	$m_i = 22$
	$m_b = 10.7$
	$s = 0.108$
	$m_r = 1$
	$s_r = 0.001$

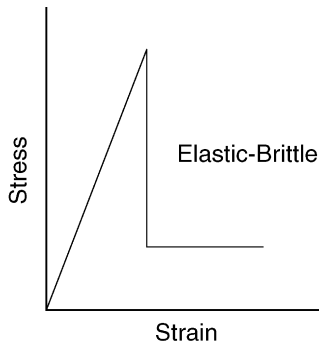

Fig. 5. Illustration of the suggested post-failure characteristic for a very good quality hard-rock mass.

Hoek and Brown [15] suggested that for good-quality rock masses the progressive spalling and slabbing nature of the failure process should be treated in an elastic−brittle manner as shown in Fig. 5. This failure process involves significant dilation, and provided there is support to the broken pieces, it is assumed that the failed rock behaves as a cohesionless frictional material. The post-peak Hoek−Brown parameters (m_r, s_r) provided in the Table 2, reflect this assumption.

The original Elliot Lake pillar-database used by Hedley and Grant [3] to establish Eq. (2) is shown in Fig. 6. Pritchard and Hedley [18] described the progressive spalling and slabbing nature of the failure process of the pillars at these mines and highlighted the difficulty of determining when a pillar had failed. Hedley and Grant [3] classified their pillars as "crushed", "partial failure" and "stable" to reflect the progressive nature of hard-rock pillar failures, and used elastic analyses to determine the loads on the pillars. An example of a "crushed" pillar is given in Fig. 7. Hence, the elastic loads for the "partial failure" or "crushed"

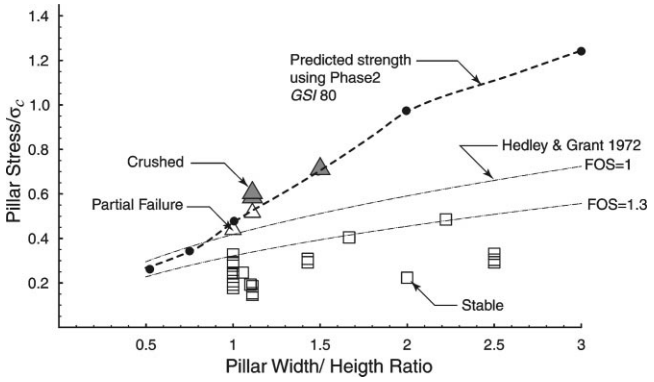

Fig. 6. Comparison of the predicted rib-pillar strength using Eq. (2) and the observed rib-pillar behavior in the Elliot Lake uranium mines. Data from Hedley and Grant [3].

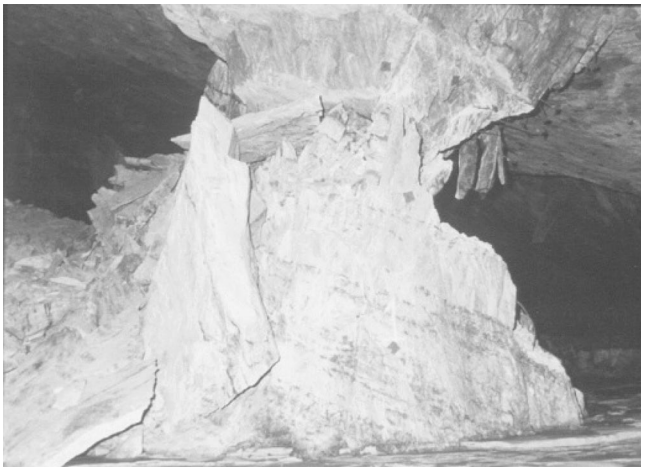

Fig. 7. Photo of a "crushed" pillar in massive quartzite, courtesy of Mr. C. Pritchard.

pillars shown in Fig. 6 are not the actual loads because once failure initiates the loads are redistributed internally within the pillar and/or to adjacent pillars. Numerical analyses were carried out to determine if the pillar strengths predicted using the Hoek–Brown failure criterion with the parameters in Table 2 were similar to the strength predicted by Eq. (2) in Fig. 6.

The numerical analyses were carried out using the two-dimensional finite element program Phase2.[1] This program has the capability to incorporate the elastic–brittle post peak response using the Hoek–Brown parameters. A pillar was considered to have failed when the elements across the pillar had yielded (Fig. 8). This was considered similar to the "crushed" conditions in Fig. 6. However, in order to compare the stress to strength ratio from the numerical program to the data in Fig. 6, the elastic stresses had to be determined for the

[1] Available from RocScience Inc. 31 Balsam Ave., Toronto, Ontario, Canada M4E 3B5; Internet:www.rocscience.com

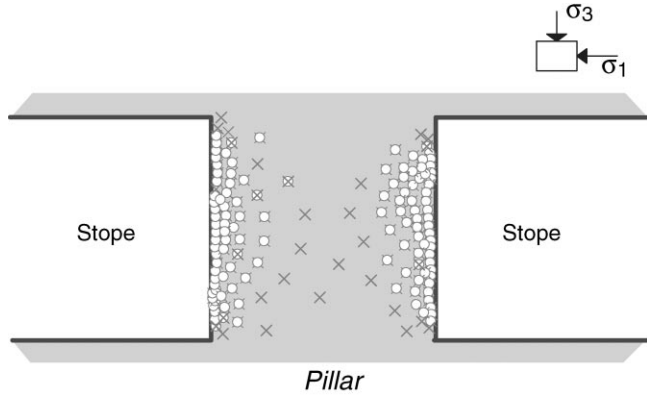

Fig. 8. Example of the output from Phase2 showing complete yielding of a pillar with a W/H ratio of 1. The × represents shear failure and the ° represents tensile failure.

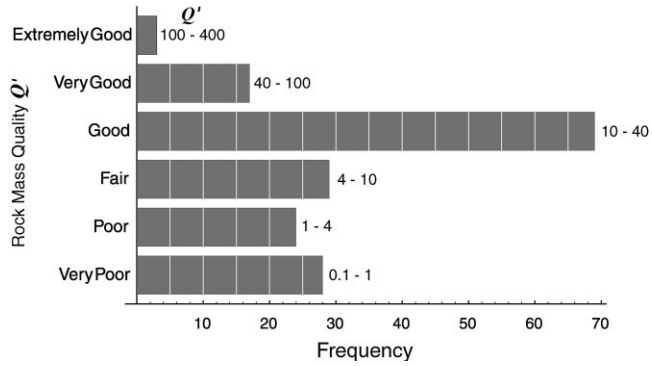

Fig. 9. Distribution of the rock mass quality Q' in Canadian hard-rock mines, data from Potvin et al. [6].

elastic–brittle failure conditions. These results are presented in Fig. 6 and agree with the failed observations for the pillar W/H ratio from 0.5 to 1.5. Beyond a pillar W/H ratio of 1.5 the elastic–brittle response appears to over predict the pillar strength compared to Eq. (2).

4. Pillar stability criterion and *GSI*

The Phase2 modelling for the Elliot Lake case study used the **GSI** for a very good-quality rock mass. In the hard-rock mines of the Canadian Shield experience suggests that the *GSI* will vary significantly. Potvin et al. [6] collected 177 case studies from Canadian hard-rock mines and found that Q' ranged from 0.1 to 120 (Fig. 9). The *GSI* values, using Eq. (6) and Potvin et al. [6] database are shown in Fig. 10. The *GSI* values range from 31 (fair) to 87 (very good) with a mean value of 67, suggesting that the *GSI* values of 40 (fair), 60 (good) and 80 (very good) would represent the range of typical strength conditions for Canadian hard-rock mines. The

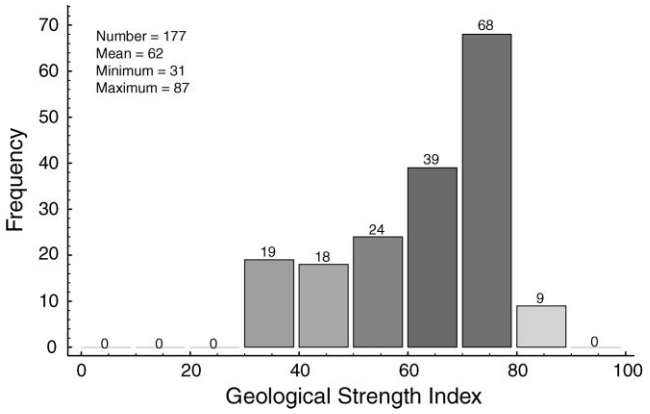

Fig. 10. Distribution of the Geological Strength Index (*GSI*) in Canadian hard-rock mines.

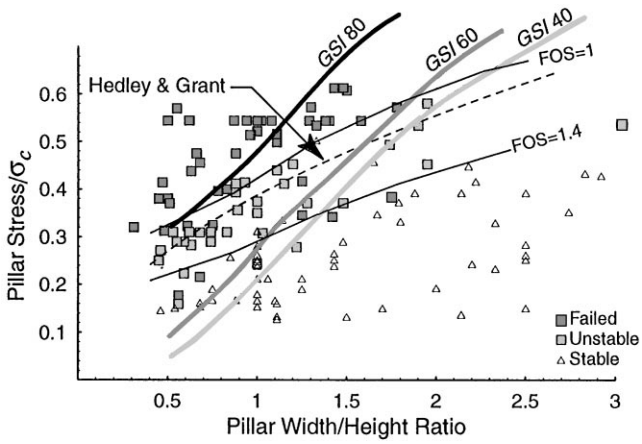

Fig. 11. The Pillar Stability Graph developed by Lunder and Pakalnis [8] compared to the pillar strength equation proposed by Hedley and Grant [3] and the Phase2 modeling results indicated by *GSI* values of 40, 60 and 80.

Table 3
GSI and Hoek–Brown strength parameters used in the Phase2 modeling.

	GSI		
	80	60	40
σ_{ci} (MPa)	230	230	230
m_i	22	22	22
m_b	10.77	5.27	2.58
s	0.108	0.0117	0.0013
Residual			
m_r	1	1	1
s_r	0.001	0.001	0.001

corresponding Hoek–Brown parameters for these strength conditions, using Eq. (8) and (9), are given in Table 3. Experience suggests that $m_i = 22$ and $\sigma_{ci} = 230$ MPa are typical values for the hard-rocks found in many Canadian underground mines.

The most extensive database of hard-rock pillar failures was compiled by Lunder and Pakalnis [8] who analyzed 178 case histories from hard-rock mines, 98 of which were located in the Canadian Shield (Fig. 11). Many of these pillars were rib or sill pillars from steeply dipping ore bodies. Lunder and Pakalnis proposed that the pillar strength could be adequately expressed by two factor of safety (*FOS*) lines. Pillars with a $FOS < 1$ fail while those with a $FOS > 1.4$ are stable. The region between $1 < FOS < 1.4$ is referred to as unstable and pillars in this region are prone to spalling and slabbing but have not completely failed, similar to the "partial failure" used by Hedley and Grant [3]. It should be noted that of the pillars investigated 76 were classed as stable; 62 were classed as failed; and 40 were classed as unstable (see Fig. 1). For comparison purposes, the Hedley and Grant pillar strength equation is also shown in Fig. 11.

Phase2 numerical analyses were carried out using the same procedure discussed in the Elliot Lake case study to develop pillar stability lines based on the rock mass strength. The Hoek–Brown parameters for *GSI* 40, 60 and 80 given in Table 3 were considered to be representative of the variation of rock mass strength found in Canadian hard-rock mines. The results from this Phase2 modelling are also shown in Fig. 11. While the Hedley and Grant pillar strength equation is in good agreement with the stability lines proposed by Lunder and Pakalnis [8], Phase2 modelling results using the Hoek–Brown failure criterion for *GSI* 40, 60 and 80 do not follow the trends of the stability lines proposed by Hedley and Grant [3] or Lunder and Pakalnis [8]. In particular, the slope of the stability lines predicted by the empirical formulas for $W/H < 1$ tend to be somewhat flat and for $W/H = 0.5$ the empirical formulas indicate that the pillar strength ranges from 0.2 to $0.35\sigma_c$. The slope of *GSI* lines, however, tend to be steeper and for $W/H = 0.5$ indicate a pillar strength ranging from 0.05 to $0.33\sigma_c$. The generally steeper slope of the *GSI* lines reflect the effect of increasing confinement, e.g., see Fig. 3, on the rock mass strength while the observed failure lines appear to be less dependent on confinement. This noticeable trend would suggest that the confining stress-dependent frictional strength component contributes less to the overall pillar strength than the conventional Hoek–Brown failure envelop predicts. However, only with additional case studies can the overall importance of the noted difference in these trend lines be fully assessed.

5. Pillar failure and cohesion loss

The failure of hard-rock pillars involves spalling, i.e., slabbing and fracturing, which leads to the progressive deterioration of the pillar strength. Pritchard and

Hedley [18] noted that in the early (pre-peak strength) stages of pillar failure at Elliot Lake stress-induced spalling, dominated the failure process while in the latter stages (post-peak strength), after spalling had created the typical hour-glass shape, slip along structural features such as bedding planes and joints played a more significant role in the failure process. These observations are in keeping with the laboratory findings of Hudson et al. [10] and Martin and Chandler [19], who demonstrated that the development of the shear failure plane occurs after the peak strength is reached. Martin [20] proposed that this pre-peak stress-induced spalling/fracturing-type failure is fundamentally a cohesion-loss process and Martin et al. [21] suggested that in order to capture this process in numerical models the Hoek–Brown parameters needed to be modified. They proposed that this spalling- or brittle-type failure could adequately be captured using elastic models and the following Hoek–Brown brittle parameters:

$$m_b = 0 \quad \text{and} \quad s = 0.11.$$

The fundamental assumption in using these brittle parameters is that the failure process is dominated by cohesion loss associated with rock mass fracturing, and that the confining stress-dependent frictional strength component can be ignored when considering near surface failure processes. Hence, it is not applicable to conditions where the frictional strength component can be mobilized and dominates the behavior of the rock mass.

A series of elastic numerical analyses were carried out using the boundary element program Examine2D[1] and the Hoek–Brown brittle parameters to evaluate pillar stability over the range of pillar W/H ratios from 0.5 to 3. The analyses were carried out using a constant k ratio of 1.5 and the results are presented as solid lines in Fig. 12 for both a factor of safety (FOS) equal to 1 and 1.4. A pillar was considered to have failed when the core of the pillar had a $FOS = 1$. A similar approach was used to establish when the pillar reached a $FOS = 1.4$. Fig. 12 shows a better agreement between the FOS lines predicted using the Hoek–Brown brittle parameters, and the FOS lines empirically developed by Lunder and Pakalnis [8] and Hedley and Grant [3] for pillar W/H ratio less than 1.5. More importantly in contrast to the failure envelopes developed using the Geological Strength Index and the traditional Hoek–Brown parameters (see Fig. 11), the slope of the failure envelope using the Hoek–Brown brittle parameters is in closer agreement with the empirical failure envelopes, particularly for pillar W/H ratios from 0.5 to 1.5. Also note that for the pillar W/H ratio less than 1, the strength is essentially constant, reflecting the low confinement for these slender pillars.

Fig. 13 shows the comparison of all the empirical formulas listed in Table 1 with the numerical results

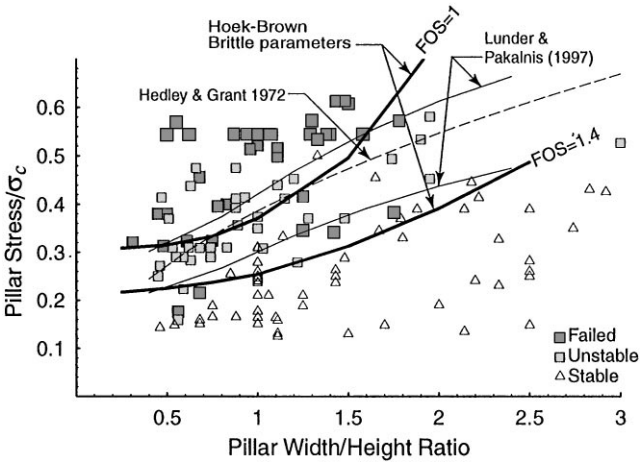

Fig. 12. Comparison of the pillar stability graph and the Phase2 modeling results using the Hoek–Brown brittle parameters.

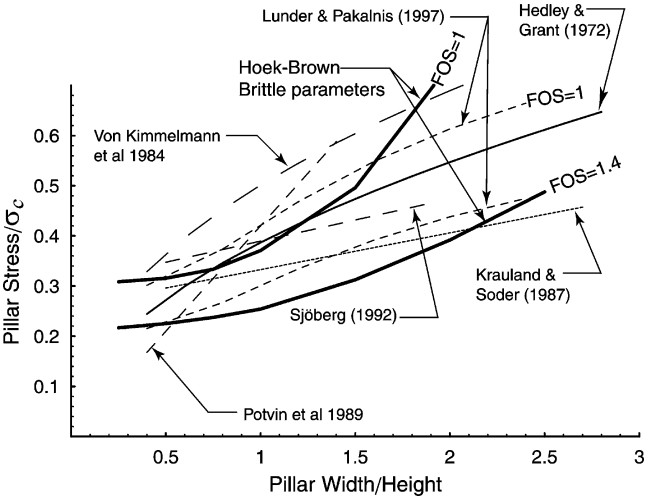

Fig. 13. Comparison of hard-rock pillar stability formulas and the elastic two-dimensional modeling results using the Hoek–Brown brittle parameters.

using the Hoek–Brown brittle parameters. There is general agreement with the empirical formulas and the predicted pillar strength for $W/H < 1.5$ where the majority of the pillar failure occur. Beyond a pillar $W/H > 2$ the Hoek–Brown brittle parameters suggest that the strength increases significantly which is in contrast to the empirical formulas. Because at pillar $W/H > 2$ the confinement at the core of the pillar is increasing significantly the use of Hoek–Brown brittle parameters will be less appropriate. It should be noted that the pillar-failure database shows that there are only a few pillar failures for pillar $W/H > 2$ (Fig. 1). Hence, the empirical pillar strength formulas should be limited to pillar $W/H < 2$.

6. Conclusions

Observations [8] of 178 pillar case studies in hard-rock mines indicate that the nearly all failures occur when the pillar W/H ratio is less than 2.5 and that the dominant mode of failure is progressive slabbing and spalling which eventually leads to an hour-glass shape. The Lunder and Pakalnis pillar stability graph documents over 98 rib-pillar observations in Canadian hard-rock mines and is based on the calculated average maximum stress in the pillar, the uniaxial strength of the intact rock and the pillar W/H ratio. Their findings are in keeping with other pillar formulas developed for hard-rock pillars and suggest that for slender pillars ($W/H<1$) failure initiates at approximately $\frac{1}{3}$ of the laboratory uniaxial compressive strength. For squat pillars ($W/H>1.5$) these empirical formulas only predict an increase in pillar strength to approximately $\frac{1}{2}$–$\frac{2}{3}$ of the laboratory uniaxial compressive strength, despite asignificant increase in confinement at the core of the pillar.

The conventional Hoek–Brown failure envelope is based on a cohesive strength component and a confining stress-dependent frictional component. In a confined state, such as pillar W/H ratios greater than 1, the frictional strength component increases significantly. Two-dimensional finite element analyses using conventional Hoek–Brown parameters for typical hard-rock rib-pillars (*GSI* of 40, 60 and 80) predicted pillar-failure envelopes that did not agree with the observed empirical failure envelopes. It is suggested that the conventional Hoek–Brown failure envelopes over predict the strength of the hard-rock pillars because the failure process is fundamentally controlled by a cohesion-loss process and for practical proposes the frictional strength component can be ignored at pillar width-to-height ratios less than 1.5.

Two-dimensional elastic analyses were carried out using the Hoek–Brown brittle parameters ($m_b=0, s=0.11$). The predicted rib-pillar strength curves were generally found to be in agreement with the observed empirical failure envelopes. It should be noted however, that the Hoek–Brown brittle parameters are not applicable to conditions where the frictional component of the rock-mass strength can be mobilized and dominates the behavior of the rock mass.

Acknowledgements

This work was supported by the Natural Sciences and Engineering Research Council of Canada (NSERC) and through collaboration with the hard-rock mining industry in Northern Ontario.

References

[1] Salamon M. Strength of coal pillars from back-calculation. In: Amadei B, Kranz RL, Scott GA, Smeallie PH, editors. Proceedings of 37th US Rock Mechanics Symposium, Vail, volume 1. Rotterdam: A.A. Balkema, 1999. p. 29–36.

[2] Sakurai S. Back analysis in rock engineering. In: Hudson JA, editor. Comprehensive rock engineering–excavation, support and monitoring, vol. 4. Oxford: Pergamon Press, 1993. p. 543–69.

[3] Hedley DGF, Grant F. Stope-and-pillar design for the Elliot Lake Uranium Mines. Bull Can Inst Min Metall 1972;65:37–44.

[4] Von Kimmelmann MR, Hyde B, Madgwick RJ. The use of computer applications at BCL Limited in planning pillar extraction and design of mining layouts. In: Brown ET, Hudson JA, editors. Proceedings of ISRM Symposium: Design and Performance of Underground Excavations. London: British Geotechnical Society, 1984. p. 53–63.

[5] Krauland N, Soder PE. Determining pillar strength from pillar failure observations. Eng Min J. 1987;8:34–40.

[6] Potvin Y, Hudyma MR, Miller HDS. Design guidelines for open stope support. Bull Can Min Metall 1989;82:53–62.

[7] Sjöberg J. Failure modes and pillar behaviour in the Zinkgruvan mine. In: Tillerson JA, Wawersik WR, editors. Proceedings of 33rd U.S. Rock Mechanics Symposium, Sante Fe. Rotterdam: A.A. Balkema, 1992. p. 491–500.

[8] Lunder PJ, Pakalnis R. Determination of the strength of hard-rock mine pillars. Bull Can Inst Min Metall 1997;90:51–5.

[9] Salamon MDG, Munro AH. A study of the strength of coal pillars. J S Afr Inst Min Metall 1967;68:55–67.

[10] Hudson JA, Brown ET, Fairhurst C. Shape of the complete stress-strain curve for rock. In: Cording E, editor. Proceedings of 13th US Symposium on Rock Mechanics, Urbana. New York: American Society of Civil Engineers, 1972. p. 773–95.

[11] Madden BJ. A re-assement of coal-pillar design. J S Afr Inst Min Metall 1991;91:27–36.

[12] Hedley DGF, Roxburgh JW, Muppalaneni SN. A case history of rockbursts at Elliot Lake. In: Proceedings of 2nd International Conference on Stability in Underground Mining, Lexington. New York: American Institute of Mining, Metallurgical and Petroleum Engineers, Inc., 1984. p. 210–34.

[13] Hoek E, Brown ET. Underground excavations in rock. London: The Institution of Mining and Metallurgy, 1980.

[14] Maybee WG. Pillar design in hard brittle rocks. Master's thesis, School of Engineering, Laurentian University, Sudbury, ON, Canada, 1999.

[15] Hoek E, Brown ET. Practical estimates of rock mass strength. Int J Rock Mech Min Sci. 1997;34:1165–86.

[16] Coates DF, Gyenge M. Incremental design in rock mechanics. Monograph, vol. 880. Ottawa: Canadian Government Publishing Centre, 1981.

[17] Barton N, Grimstad E. The Q-System following twenty years of application in NWT support selection. Felsbau, 1994;12:428–36.

[18] Pritchard CJ, Hedley DGF. Progressive pillar failure and rockbursting at Denison Mine. In: Young RP, editor. Proceedings of 3rd International Symposium on Rockbursts and Seismicity in Mines, Kingston. Rotterdam: A.A. Balkema, 1993. p. 111–6.

[19] Martin CD, Chandler NA. The progressive fracture of Lac du Bonnet granite. Int J Rock Mech Min Sci Geomech Abstr 1994;31:643–59.

[20] Martin CD. Seventeenth Canadian Geotechnical Colloquium: the effect of cohesion loss and stress path on brittle rock strength. Can Geotech J 1997;34:698–725.

[21] Martin CD, Kaiser PK, McCreath DR. Hoek-Brown parameters for predicting the depth of brittle failure around tunnels. Can Geotech J 1999;36:136–51.